Original Research

Identification and analysis of immune-related subtypes of hepatocellular carcinoma

Qimeng Wang[1,*], Jin Huang[2,*], Huihua Zhang[3], Huan Liu[4,5] and Min Yu[1]

[1]Department of General Surgery, Xinqiao Hospital, Army Medical University, Chongqing 400037, China; [2]Department of Clinical Laboratory, Wuhan Fourth Hospital, Puai Hospital, Tongji Medical College, Huazhong University of Science and Technology, Wuhan 430000, China; [3]Department of Gastroenterology, Children's Hospital of Chongqing Medical University, Chongqing 400014, China; [4]Department of Orthopaedics, Affiliated Traditional Chinese Medicine Hospital, Southwest Medical University, Luzhou 646000, China; [5]Guangdong Innovation Platform for Translation of 3D Printing Application, The Third Affiliated Hospital of Southern Medical University, Guangzhou 510000, China

Corresponding authors: Min Yu. Email: yumimianbao@163.com; Huan Liu. Email: 20016040@163.com

*These authors contributed equally to this work.

Impact statement

In this study, we classified hepatocellular carcinoma (HCC) into three subtypes, namely Immunity_M, Immunity_L, and Immunity_H. The immune signature analysis of the three subtypes verified that Immunity_H displayed high immune activity. Further function analysis involving the differentially expressed genes (DEGs) of Immunity_L and Immunity_H revealed that they exhibited a substantial correlation with immune-related pathways. The DEGs such as B2M, HLA-DRA, HLA-DRB1 may be used as potential markers that distinguish the immune subtypes of HCC. Moreover, our results suggest that application of immune checkpoint inhibitors or other immunotherapies in the Immunity_H group may yield better benefits, and this could also provide a basis for the individualized immunotherapy of HCC.

Abstract

Hepatocellular carcinoma is a malignance that remains difficult to cure. Immunotherapy has shown its potential application in a variety of refractory malignancies. Due to the complexity of immune microenvironment of hepatocellular carcinoma, the efficacy of immunotherapy for hepatocellular carcinoma is not as effective as expected. Expression data of hepatocellular carcinoma from the TCGA and ICGC databases were used for classification and verification of hepatocellular carcinoma subtypes. The immune-related functions and pathways were identified via gene set enrichment analysis, while the sections denoting the subsets of the immune cells were estimated using the CIBERSORT algorithm. Immunity low (Immunity_L), immunity medium (Immunity_M), and immunity high (Immunity_H) were specified as the three immune-related subtypes of hepatocellular carcinoma. The quantity of stromal and immune cells was the most substantial in Immunity_H, compared to the other subtypes. Interestingly, the proportion of M0 macrophages decreased from Immunity_L to Immunity_H, while the proportion of CD8 T cells increased. Furthermore, the HLA genes expression levels, as well as those of six immune checkpoint genes were substantially lower in Immunity_L than in Immunity_H. Functional analysis was performed for 1512 differentially expressed genes between Immunity_L and Immunity_H. Finally, the PPI network was constructed with 118 nodes. The highest connectivity degree nodes were B2M, HLA-DRA, and HLA-DRB1. The above results were verified in ICGC-JP and ICGC-FR databases with a consistent trend. In this study, we divided hepatocellular carcinoma into three subtypes and explored the immune-related characteristics of these subtypes. These results may provide new insights for immunotherapy of hepatocellular carcinoma.

Keywords: Hepatocellular carcinoma, immunotherapy, immune-related subtypes, immune genes, biomarker

***Experimental Biology and Medicine* 2021; 246: 667–677. DOI: 10.1177/1535370220970130**

Introduction

As the most prevalent primary live cancer and the fifth most common cancer, hepatocellular carcinoma (HCC) denotes the second highest causative factor for cancer-associated fatality in malignancies globally, while the occurrence and development of HCC are closely related to hepatitis B or C virus infection or alcohol abuse.[1,2] Traditional treatments for HCC include radiofrequency ablation (RFA), radiotherapy, transcatheter hepatic arterial chemoembolization (TACE), and surgery.[3] Actually, these treatments offer only modest benefits in terms of overall survival and the response of HCC patients to them is not satisfactory. For instance, TACE or radioembolization is used to treat multinodular intermediate stage HCC, but

the overall survival is usually less than 20 months.[4–6] Furthermore, systemic chemotherapy has been ineffective for treating HCC patients due to inherent hepatocyte chemoresistance.[7]

In recent years, immunotherapy has received increasing attention. Various studies have shown that the use of the anti-PD-1, anti-PD-L1, and anti-CTLA-4 immune checkpoint inhibitors can regulate tumor growth, increasing the survival of patients, while substantially decreasing the cancer recurrence risk following surgery and transplantation.[8,9] However, HCC has been reported to be a tumor type with low/moderate immunogenicity.[10] HCC cells are in a highly immunosuppressive microenvironment, which can cause host immunosuppression by down-regulating the major histocompatibility complex I (MHC-I) molecule, secreting immunosuppressive cytokines, and mediating negative co-stimulatory signals to escape the autoimmune response.[11] Accordingly, immunotherapy exhibits a modest treatment efficacy in HCC. Considering the complexity and diversity of the immune microenvironment of HCC, there is an urgent need to classify HCC subtypes on the basis of immune characteristics so as to provide a theoretical basis for precise and individualized immunotherapy.

Here, the HCC information obtained from The Cancer Genome Atlas (TCGA) database was analyzed and divided HCC into Immunity_M, Immunity_H, and Immunity_L subtypes, the immune signatures of which were analyzed, while the functions of the DEGs in Immunity_L and Immunity_H were investigated.

Materials and methods

HCC sample databases

The TCGA database (https://cancergenome.nih.gov/) was used to retrieve the gene expression profiles of 347 cases of HCC, while the genes with expression levels greater than 0 in each sample accounting for more than 30% of the genes were identified in the immune gene set. All the patients were at stages I–IV, and only patients with detailed follow-up information were included. The demographic details and characteristics of all HCC samples are listed in Table S1. The external validation cohort included 389 HCCs (158 ICGC_FR and 231 ICGC_JP) which were collected by the ICGC database (https://icgc.org/). The flow chart of the study is shown in Figure 1.

Gene expression data preprocessing

The Illumina platform was used to analyze the RNA-sequencing data. The Fragments Per Kilobase of transcript per million Mapped reads upper quartile (FPKM-uq) was acquired using the TCGA Data and ICGC Data Portal, and the Ensemble database was used for gene annotation. The value of the gene expression was further investigated after log2 transformation.

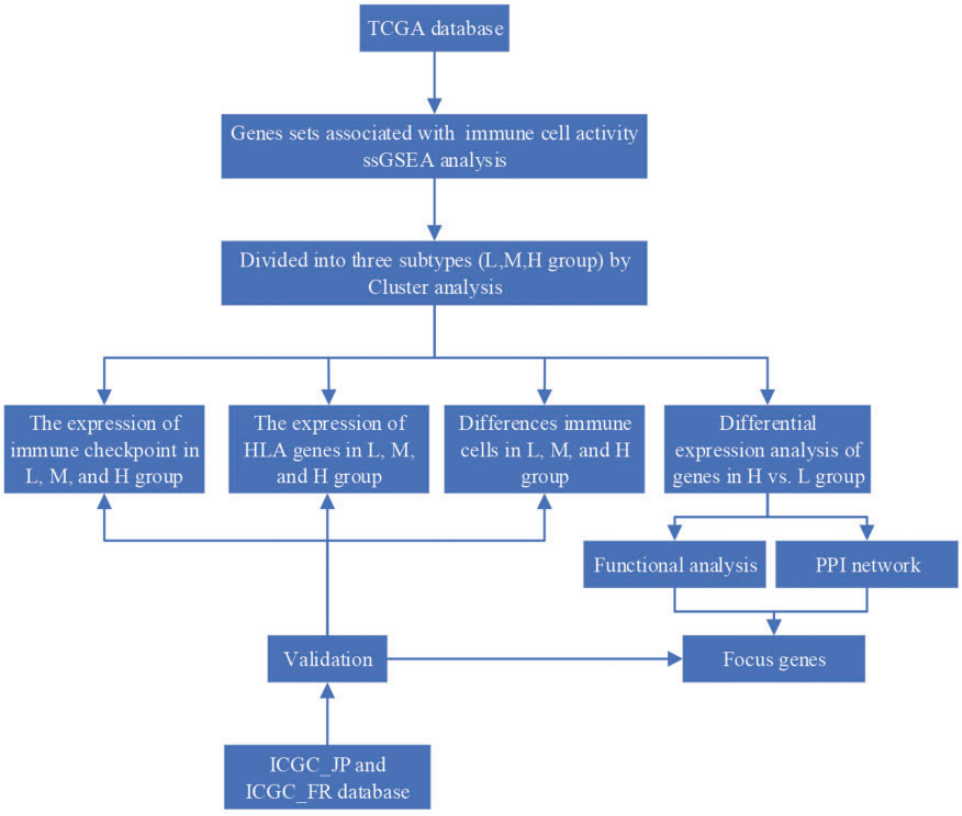

Figure 1. A flow chart of the study. HCC was classified into Immunity_M, Immunity_L, and Immunity_H subtypes by immunogenomic profiling based on the RNA-sequencing data acquired from the TCGA database. Subsequently, we analyzed the differences of immune-related genes and cells in these three subtypes and verified them in ICGC-JP and ICGC-FR databases. We then performed functional analysis and PPI network on differentially expressed genes between Immunity_H and Immunity_L to screen for focus genes. (A color version of this figure is available in the online journal.)

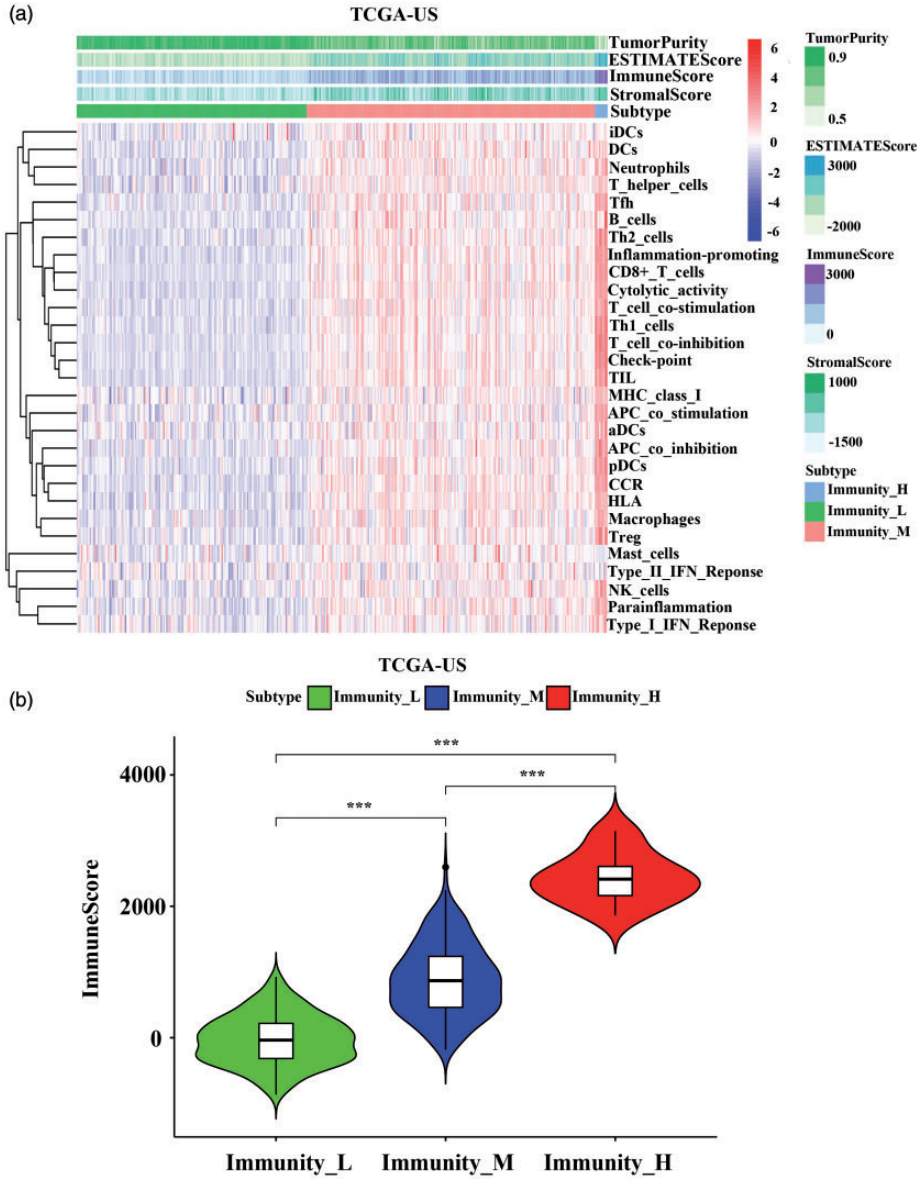

Figure 2. Identification of three HCC subtypes and evaluation of infiltrating cells and tumor purity. (a) Hierarchical clustering of HCC in the TCGA database, as well as the stromal and immune score assessment and tumor purity evaluation using ESTIMATE. Immunity_H, Immunity_M, and Immunity_L. (b) Comparing the immune scores of the three subtypes of HCC. ***$P < 0.001$. (A color version of this figure is available in the online journal.)

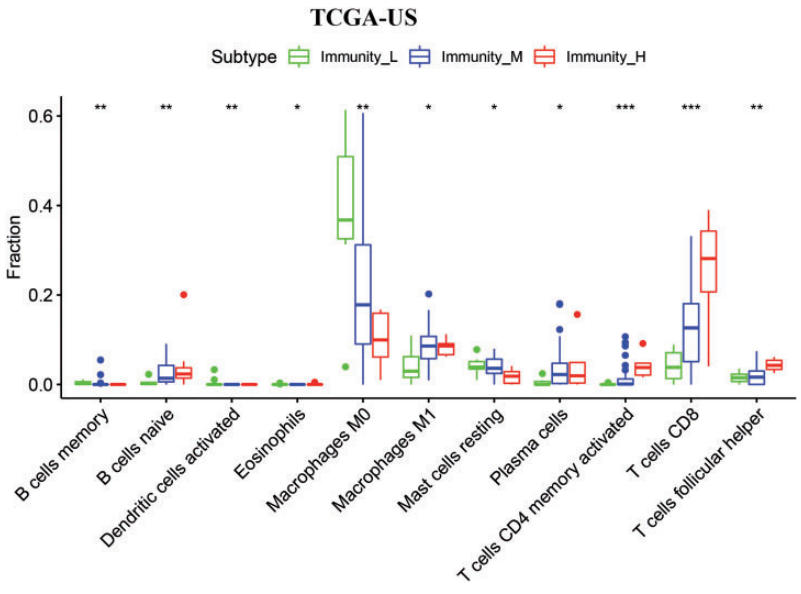

Figure 3. An analysis of the proportion of the immune cells in the subtypes of HCC. Eleven immune cells subsets with significant differences among the three subtypes were listed. *$P < 0.05$, **$P < 0.01$, ***$P < 0.001$. (A color version of this figure is available in the online journal.)

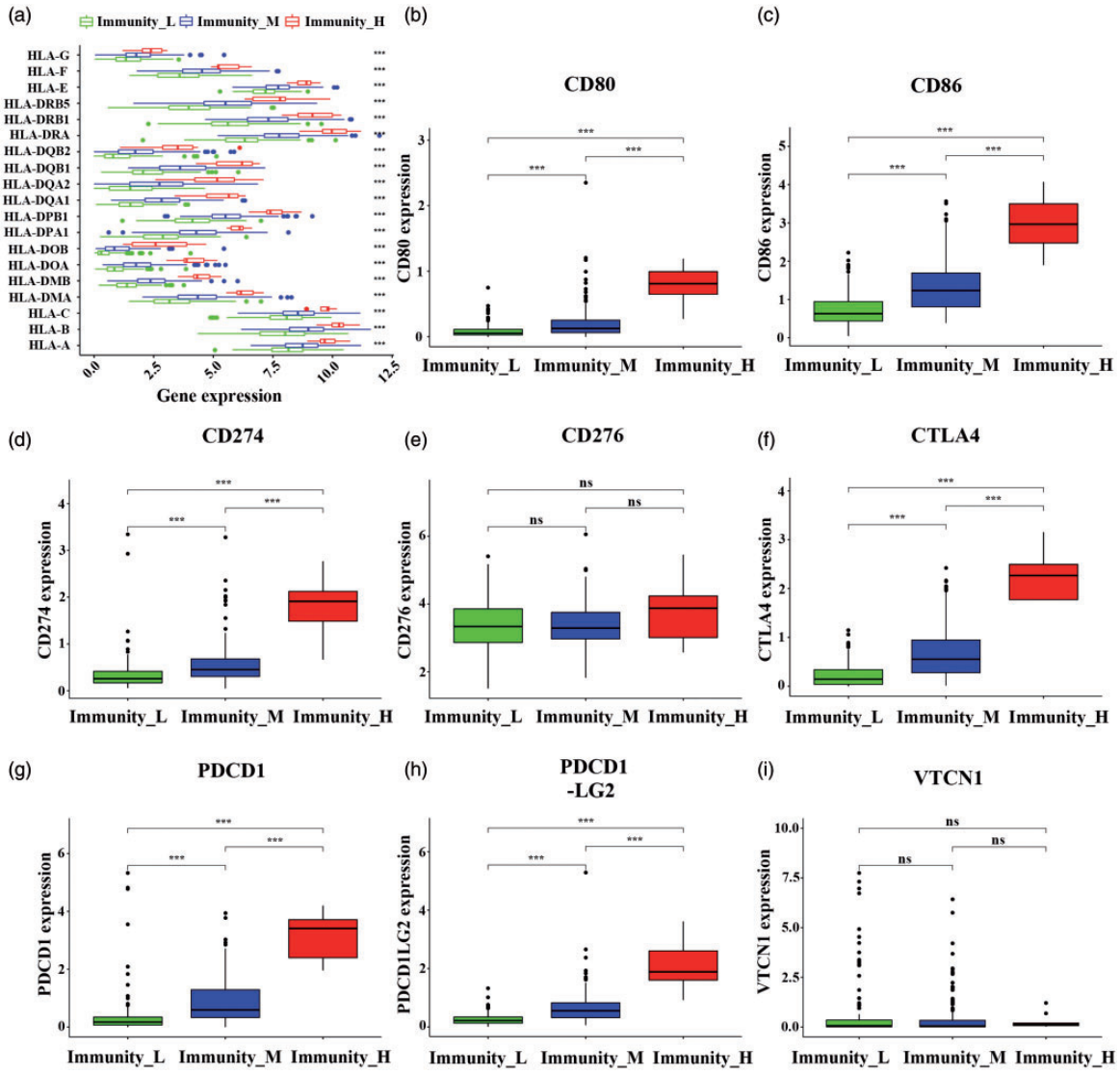

Figure 4. An assessment of the immune gene expression levels in the three subtypes of HCC. (a) Comparing the gene expression levels of HLA in the three HCC subtypes. (b–i). The expression levels of eight immune checkpoint genes in the three HCC subtypes. ***$P < 0.001$, ns: none sense. (A color version of this figure is available in the online journal.)

Hierarchical cluster analysis

Here, the levels of enrichment of 29 immune signatures were evaluated in each HCC sample using the single-sample Gene Set Enrichment Analysis (ssGSEA) score, after which hierarchical cluster analysis was conducted.[12,13]

Evaluation of infiltrating cells and tumor purity in HCC

The permeation of immune cells into the tissue of the tumor, as well as the stromal presence and tumor purity were assessed via Estimation of Stromal and Immune cells in Malignant Tumor tissues using Expression data (ESTIMATE).[14]

Comparing the proportional subsets of the immune cells among the HCC subtypes

Here, the Cell-type Identification by Estimating Relative Subsets of RNA Transcripts (CIBERSORT) resource (http://cibersort.stanford.edu/) was used to identify 22 proportional subsets of human immune cells, while using an algorithm with 1000 permutations.[15] $P < 0.05$ was used as the standard for successfully deconvoluting the samples and was considered qualified for subsequent assessment. This study employed the Mann–Whitney U to compare the immune cell subsets proportions among the HCC subtypes.

Functional enrichment analysis

A total of 21,999 mRNAs were differentially analyzed among Immunity_L and Immunity_H in the TCGA. GSEA[16,17] was performed to identify the potentially functional systems of the differential expression genes ($|\log FC| > 2$, and false discovery rate (FDR) < 0.05) in Immunity_H and Immunity_L using GSEA 4.0 software in conjunction with the gene sets found in the Kyoto Encyclopedia of Genes and Genomes (KEGG) and Gene Ontology (GO).

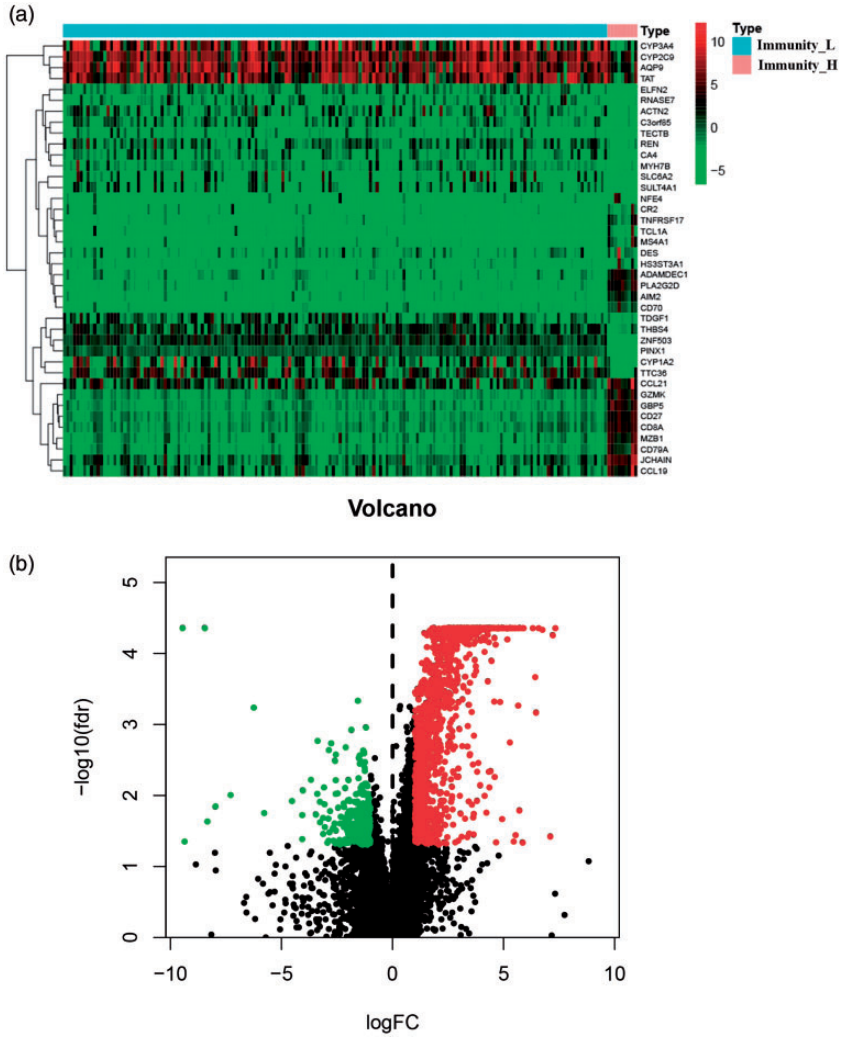

Figure 5. The DEGs of Immunity_L and Immunity_H. (a) The heatmap shows the hierarchical cluster analysis of the DEGs of Immunity_L and Immunity_H. (b) Both the down-regulated genes, denoted by the green points, and the up-regulated genes, denoted by the red points, are illustrated by the volcano plot. (A color version of this figure is available in the online journal.)

The network construction of protein–protein interaction

This study used the Search Tool for the Retrieval of Interacting Genes (STRING) database with a confidence cutoff of 0.90 to predict interaction information between proteins. Thus, the construction of the PPI network was based on the data of the STRING database, and gene degrees exceeding or equal to 10 were denoted as hub genes.

Statistical analysis

The expression values and immune scores of the checkpoint genes of the various subtypes of HCC were compared using the Student's *t*-test. Furthermore, to reduce the false positive rates, multiple testing correction was achieved using Benjamini–Hochberg's FDR. All tests were double sided, while *P*-values below 0.05 were regarded as statistically significant. Furthermore, R software version 3.5.3 (http://www.R-project.org) was employed for the execution of all statistical assessments.

Results

Identifying three HCC subtypes according to 29 immune signatures

According to the HCC expression profile data in the TCGA database, the hierarchical clustering of HCC was performed considering the levels of enrichment for 29 immune signatures (Table S2). The heatmaps showed the visible segregation of three clusters (Figure 2(a)), which were defined as Immunity_M, Immunity_L, and Immunity_H, respectively. The result was verified in the other two databases (ICGC-JP and ICGC-FR) (Figure S1).

Evaluation of the infiltrating cells, as well as tumor purity in the three subtypes of HCC

As shown in Figure 2(a), the immune and stromal scores of Immunity_H surpassed that of Immunity_L. Furthermore, Immunity_H displayed lower tumor purity than Immunity_L. In addition, Figure 2(b) also indicated that

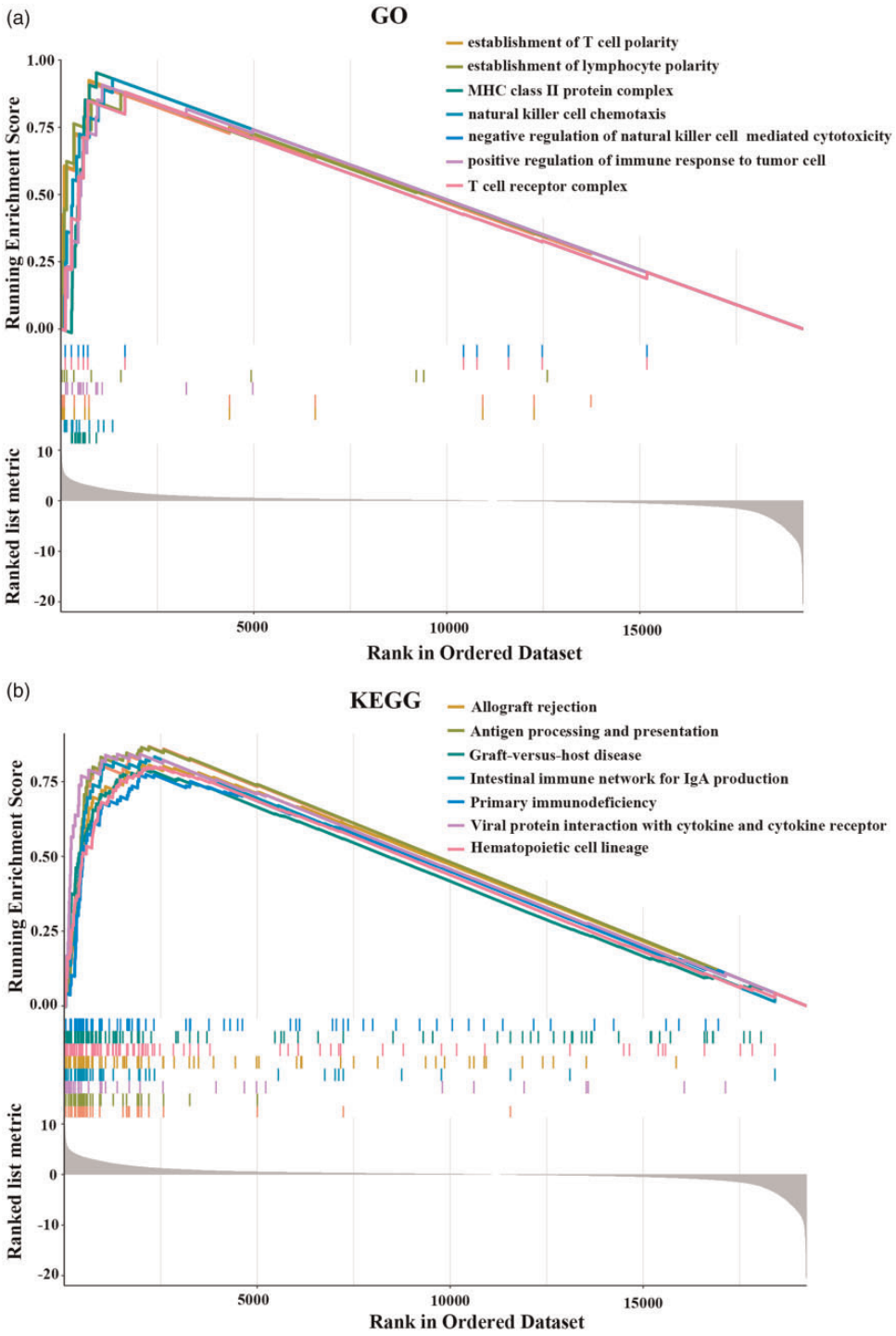

Figure 6. Functional analysis of DEGs between Immunity_H and Immunity_L. (a) TOP 7 of GO enrichment. (b) TOP 7 of KEGG pathway enrichment. (A color version of this figure is available in the online journal.)

Immunity_H had a significantly higher immune score than Immunity_L and Immunity_M. The results were analyzed according to the data in the TCGA database and verified in the ICGC-JP and ICGC-FR databases (Figure S2). These results indicated that compared with Immunity_L, the number of stromal and immune cells was significantly increased in Immunity_H.

A comparison of the immune cell fraction in the three HCC subtypes

CIBERSORT was employed to investigate the relative proportion of 22 immune cell subsets in different subtypes of HCC samples in the TCGA database, and 11 immune cells subsets with significant differences among the three groups are listed in Figure 3. Among the 11 subsets of tumor-

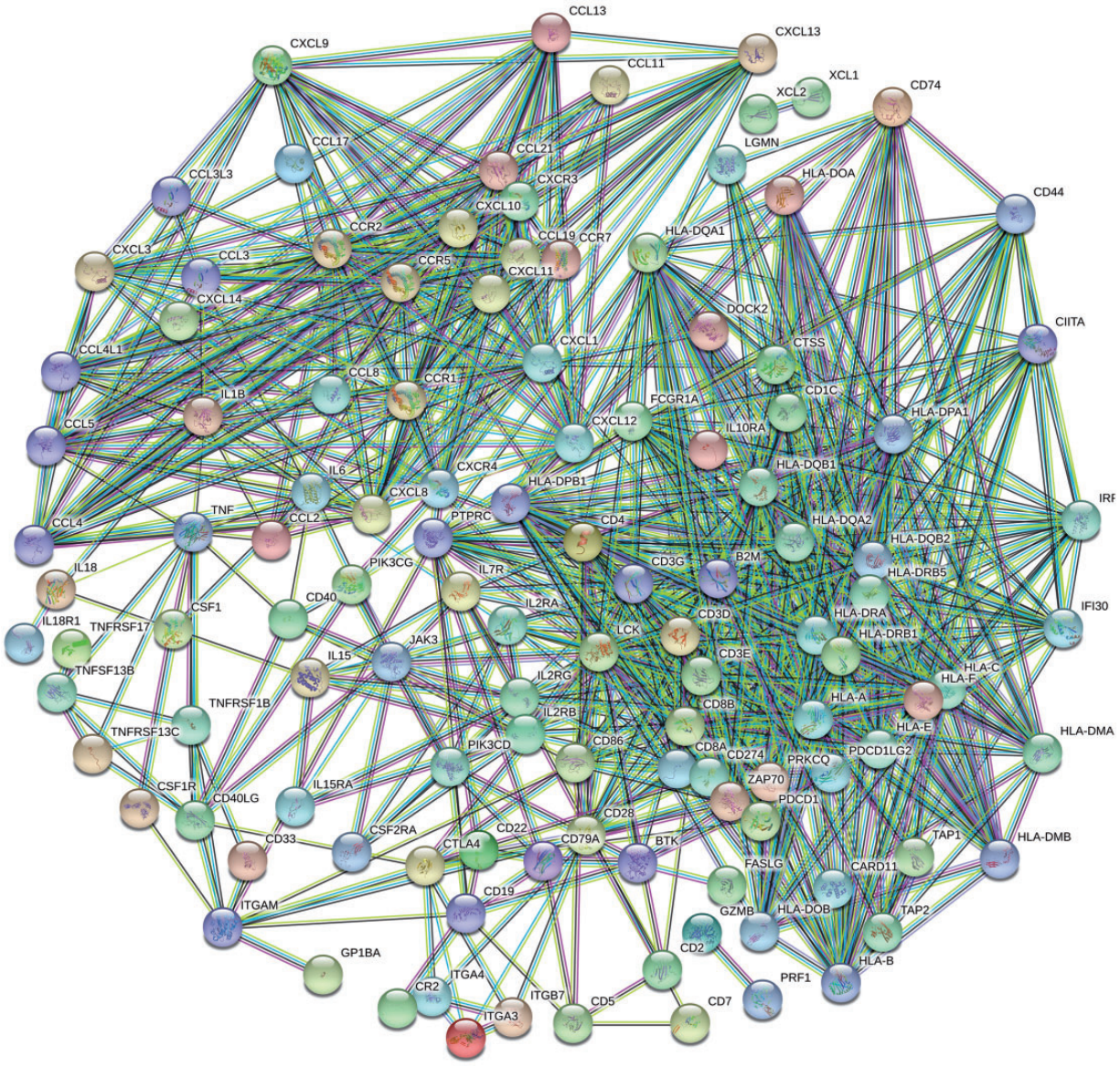

Figure 7. The construction of the PPI network. The associated DEGs of the TOP 7 pathways in the KEGG and GO enrichment analyses, respectively, were selected to construct the PPI network. Each circle represents protein-coding gene. (A color version of this figure is available in the online journal.)

infiltrating immune cells CD8 T cells and M0 macrophages account for the largest proportion, which suggests that they may play a key role during the progression of HCC. Interestingly, the proportion of M0 macrophages decreased from Immunity_L to Immunity_H, while the proportion of CD8 T cells increased. In addition, five immune cells subsets and nine immune cells subsets with significant differences among the three groups in ICGC-FR and ICGC-JP databases are listed in Figure S3.

A comparison of the immune gene expression in the three HCC subtypes

As shown in Figure 4(a), the HLA genes expression levels in Immunity_H, which include HLA-DRB5, HLA-DRB1, HLA-C, HLA-B, and HLA-A were markedly elevated compared to those in Immunity_L.

Additionally, the expression of eight immune checkpoint genes in the TCGA database was examined (Figure 4(b)). We found that Immunity_H exhibited considerably higher expression levels of CD80, CD86, CD274, CTLA4, PDCD1, and PDCD1-LG2 than Immunity_L. However, VTCN1 and CD276 expression displayed no notable differences for the Immunity_H and Immunity_L groups. These results were also confirmed in the ICGC-JP and ICGC-FR databases (Figures S4 and S5).

Functional analysis of the differentially expressed genes in Immunity_H vs. Immunity_L

Employing $P < 0.05$ and $|\text{Fold changes}| \geq 2$ as cutoffs, 1512 DEGs were acquired, which included 1269 genes that were up-regulated and 243 that were down-regulated. The heatmap and volcano plots of the DEGs are shown in Figure 5 (a) and (b). Of particular interest, the heatmap indicates a

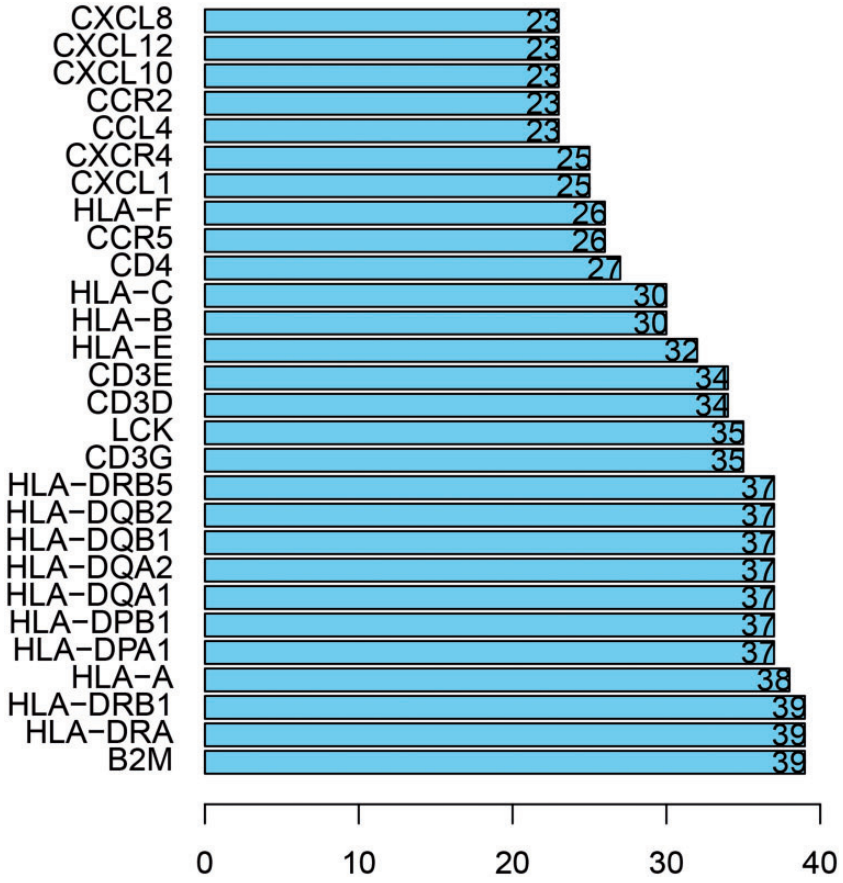

Figure 8. Top 28 high-degree hub nodes in PPI network. The x-axis shows the degree values, while the y-axis indicates the protein-coding genes. (A color version of this figure is available in the online journal.)

clear clustering boundary between Immunity_L and Immunity_H.

GSEA was conducted to analyze the enriched GO terms[18,19] and KEGG[20] pathways of the DEGs in the Immunity_H group, as well as the Immunity_L group. The top seven GSEA results including GO and KEGG are listed in Figure 6. Obviously, the DEGs highly corresponded with the immune-associated pathways, including the establishment of lymphocyte and T cell polarities, the MHC class II protein complex, allograft rejection, and antigen processing and presentation, among others. More interestingly, Table S3 shows that the DEGs involved in the top seven GSEA results were up-regulated in the group labeled Immunity_H. These results support the conclusion that the immune activity of Immunity_H group is elevated.

PPI network construction

The related DEGs of the top 7 pathways in GO enrichment analysis and KEGG analysis, respectively (Table S3), were selected for the PPI network construction, which contained 118 nodes (Figure 7). The degree values of the top 28 nodes in PPI network topology were compared, as listed in Figure 8. The highest connectivity degree nodes were B2M (degree = 39), HLA-DRA (degree = 39), and HLA-DRB1 (degree = 39).

Six genes (B2M, HLA-DRA, CCR5, CXCR4, CXCL12, and LCK) were chosen for the expression level validation in the ICGC-JP and ICGC-FR databases. As shown in Figure 9, the expression of the six Immunity_H genes substantially surpassed that of Immunity_L.

Discussion

In the present study, we focus on classifying HCC according to immune signatures. On the basis of the expression profile data of HCC in the TCGA database, three subtypes were identified as Immunity_M, Immunity_L, and Immunity_H. As HCC is known to include complex ecosystems which comprise of non-tumor cells, mainly immune-related cells,[1] the levels of infiltrating stromal and immune cells, as well as tumor purity were evaluated in the three HCC subtypes. As expected, we found a substantial elevation in the immune cell quantity in Immunity_H compared with Immunity_L.

We further explored the relative proportion of immune cell subsets in the different subtypes of HCC. The immune cell components in the microenvironment of the tumor are complex and diverse, including B lymphocytes, dendritic cells, T lymphocytes, natural killer cells, and macrophages.[21,22] Altered immune cell compositions and proportions in the microenvironment of the tumor microenvironment are essential in the occurrence and development of HCC. For instance, clinical studies illustrated the presence of a positive correlation between tumor-infiltration lymphocyte density and the prognosis

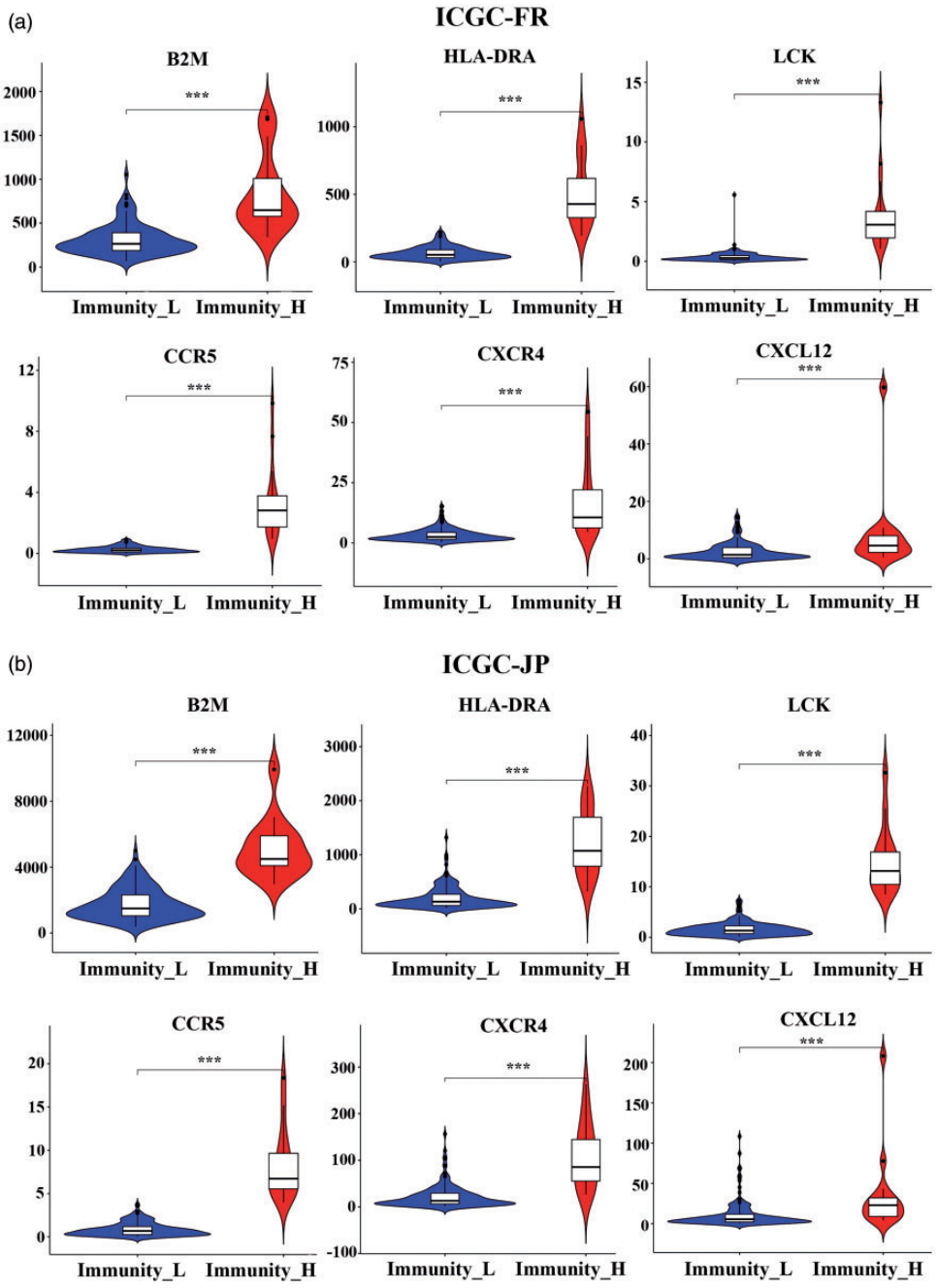

Figure 9. The validation of six immune genes in ICGC-FR (a) and ICGC-JP (b) databases. B2M, HLA-DRA, CCR5, CXCR4, CXCL12, and LCK were chosen to validate the expression levels in the ICGC-JP and ICGC-FR databases. *** $P < 0.001$. (A color version of this figure is available in the online journal.)

of cancer survival.[23,24] The tumor-associated macrophages participate in cancer progression and metastasis. M0 macrophages can be induced through polarization to transform into M1 macrophages or M2 macrophages by microenvironmental stimuli. Such M1 macrophages could exert anti-inflammatory properties, and may suppress early HCC tumorigenesis.[25] In addition, CD8 T cells have been considered as major drivers of antitumor immunity.[26] Patients with high infiltration of CD8 T cells had better overall survival.[27] The present study also revealed that the CD8 T cell and M1 macrophage proportions in Immunity_H, significantly exceeded that in Immunity_L. This result may indicate that the Immunity_H group has higher antitumor immune activity than Immunity_L.

The expression of eight immune checkpoint genes in the three subtypes of HCC was examined, revealing that the expression levels of CD80, CD86, CD274, CTLA-4, PDCD1, and PDCD1-LG2 in Immunity_H substantially exceeded those in Immunity_L. Recently, various studies have demonstrated that applying immune checkpoint inhibitors has a significant influence on the prognosis of HCC. For example, CTLA-4 is an inhibitory co-receptor that obstructs T cell activation and proliferation. Clinical research has shown that blocking CTLA-4 with tremelimumab in patients

could provide better treatment benefits.[28] In addition, studies have shown that the use of anti-PD-1 monoclonal antibodies such as Nivolumab and pembrolizumab can significantly increase the cure rate and survival time of patients.[29] Accordingly, using immune checkpoint inhibitors in Immunity_H patients may yield better benefits.

In order to further study the differences between the Immunity_L and Immunity_H groups, functions, pathways, and networks of the DEGs were analyzed. Interestingly, DEGs of the TOP seven enriched pathways in GO and KEGG function analysis respectively were all up-regulated in Immunity_H, suggesting that these signaling pathways may be activated in Immunity_H. The core genes of PPI networks contain HLAs, chemokines genes (such as CCR5, CXCR4, CXCL12, etc.), and B2M among other genes.

Chemokines are a large class of small molecule proteins with chemotaxis in the cytokine superfamily, which can be produced from various cells. Current research confirms that abnormal expression of chemokines can affect the invasive ability of tumor cells.[30,31] CXCL12 and CXCL10 are two of the most important factors in the CXCL subfamily of chemokines. Studies have shown that the expression of CXCL12 and CXCL10 in HCC tissues is significantly higher than that in adjacent tissues.[32–34] CXCR4 is an important chemokine receptor. The CXCL12/CXCR4 axis is crucial in tumor metastasis. Recent research shows that restricting the CXCR4/CXCL12 axis may directly inhibit the migration, invasion, and metastases of tumors.[35]

The B2M gene is responsible for encoding a serum protein beta-2-microglobulin that is associated with the class I heavy chain of MHC. It is vital for the formation of MHC-I complex, as well as the presentation of peptides.[36] Research has suggested that B2M gene mutations are associated with a decrease in MHC class I expression, as well as a lower patient survival rate.[37] Besides, various studies have shown that B2M can be used as an immune marker for a variety of tumors.[38,39] The expression of B2M in Immunity_L is substantially lower than that in Immunity_H, suggesting that the protein may be used as a potential immune marker in the Immunity_H group.

In conclusion, we classified HCC into subtypes denoted by Immunity_M, Immunity_L, and Immunity_H, and analyzed the immune signatures in these subtypes. Further, function analysis of the DEGs in Immunity_L and Immunity_H was performed to find potential markers that may be used to effectively identify patients with high immunity. These results may offer clinical value for immunotyping of patients with HCC and also provide a basis for individualized immunotherapy.

AUTHORS' CONTRIBUTIONS

MY and HL designed and directed the project. QW, JH, and HZ participated in the collection of data. QW and JH participated in the data analysis. QW and MY wrote the manuscript.

DECLARATION OF CONFLICTING INTERESTS

The author(s) declared no potential conflicts of interest with respect to the research, authorship, and/or publication of this article.

FUNDING

The author(s) disclosed receipt of the following financial support for the research, authorship, and/or publication of this article: This study utilized grants obtained from the National Natural Science Foundation of China (NSFC 81970468 to M.Y.), Postdoctoral Science Foundation of China (2018M643127 to H.L.), and the Technology Strategic Cooperation Project of Southwest Medical University Science and Luzhou (2018LZXNYD-ZK19 to H.L.), Applied basic research project of Wuhan Science and Technology Bureau (2019020701011472 to J. H.).

SUPPLEMENTAL MATERIAL

Supplemental material for this article is available online.

REFERENCES

1. Villanueva A. Hepatocellular carcinoma. *N Engl J Med* 2019;**380**:1450–62
2. European Association for the Study of the Liver Electronic address: easloffice@easloffice.eu; European Association for the Study of the Liver EASL clinical practice guidelines: management of hepatocellular carcinoma. *J Hepatol* 2018;**69**:182–236
3. Raoul JL, Frenel JS, Raimbourg J, Gilabert M. Current options and future possibilities for the systemic treatment of hepatocellular carcinoma. *Hepat Oncol* 2019;**6**:HEP11
4. Sangro B, Carpanese L, Cianni R, Golfieri R, Gasparini D, Ezziddin S, Paprottka PM, Fiore F, Van Buskirk M, Bilbao JI, Ettorre GM, Salvatori R, Giampalma E, Geatti O, Wilhelm K, Hoffmann RT, Izzo F, Inarrairaegui M, Maini CL, Urigo C, Cappelli A, Vit A, Ahmadzadehfar H, Jakobs TF, Lastoria S. European network on radioembolization with yttrium-90 resin M. Survival after yttrium-90 resin microsphere radioembolization of hepatocellular carcinoma across Barcelona clinic liver cancer stages: a European evaluation. *Hepatology* 2011;**54**:868–78
5. Llovet JM, Bruix J. Systematic review of randomized trials for unresectable hepatocellular carcinoma: chemoembolization improves survival. *Hepatology* 2003;**37**:429–42
6. Prieto J, Melero I, Sangro B. Immunological landscape and immunotherapy of hepatocellular carcinoma. *Nat Rev Gastroenterol Hepatol* 2015;**12**:681–700
7. Eatrides J, Wang E, Kothari N, Kim R. Role of systemic therapy and future directions for hepatocellular carcinoma. *Cancer Control* 2017;**24**:1073274817729243
8. Akateh C, Black SM, Conteh L, Miller ED, Noonan A, Elliott E, Pawlik TM, Tsung A, Cloyd JM. Neoadjuvant and adjuvant treatment strategies for hepatocellular carcinoma. *World J Gastroenterol* 2019;**25**:3704–21
9. Tian M, Shi Y, Liu W, Fan J. Immunotherapy of hepatocellular carcinoma: strategies for combinatorial intervention. *Sci China Life Sci* 2019;**62**:1138–43
10. Cristescu R, Mogg R, Ayers M, Albright A, Murphy E, Yearley J, Sher X, Liu XQ, Lu H, Nebozhyn M, Zhang C, Lunceford JK, Joe A, Cheng J, Webber AL, Ibrahim N, Plimack ER, Ott PA, Seiwert TY, Ribas A, McClanahan TK, Tomassini JE, Loboda A, Kaufman D. Pan-tumor genomic biomarkers for PD-1 checkpoint blockade-based immunotherapy. *Science* 2018;**362**:eaar3593
11. Lin CL, Kao JH. Risk stratification for hepatitis B virus related hepatocellular carcinoma. *J Gastroenterol Hepatol* 2013;**28**:10–7
12. Hanzelmann S, Castelo R, Guinney J. GSVA: gene set variation analysis for microarray and RNA-seq data. *BMC Bioinformatics* 2013;**14**:7

13. Barbie DA, Tamayo P, Boehm JS, Kim SY, Moody SE, Dunn IF, Schinzel AC, Sandy P, Meylan E, Scholl C, Frohling S, Chan EM, Sos ML, Michel K, Mermel C, Silver SJ, Weir BA, Reiling JH, Sheng Q, Gupta PB, Wadlow RC, Le H, Hoersch S, Wittner BS, Ramaswamy S, Livingston DM, Sabatini DM, Meyerson M, Thomas RK, Lander ES, Mesirov JP, Root DE, Gilliland DG, Jacks T, Hahn WC. Systematic RNA interference reveals that oncogenic KRAS-driven cancers require TBK1. *Nature* 2009;**462**:108–12
14. Yoshihara K, Shahmoradgoli M, Martinez E, Vegesna R, Kim H, Torres-Garcia W, Trevino V, Shen H, Laird PW, Levine DA, Carter SL, Getz G, Stemke-Hale K, Mills GB, Verhaak RG. Inferring tumour purity and stromal and immune cell admixture from expression data. *Nat Commun* 2013;**4**:2612
15. Newman AM, Liu CL, Green MR, Gentles AJ, Feng W, Xu Y, Hoang CD, Diehn M, Alizadeh AA. Robust enumeration of cell subsets from tissue expression profiles. *Nat Methods* 2015;**12**:453–7
16. Subramanian A, Tamayo P, Mootha VK, Mukherjee S, Ebert BL, Gillette MA, Paulovich A, Pomeroy SL, Golub TR, Lander ES, Mesirov JP. Gene set enrichment analysis: a knowledge-based approach for interpreting genome-wide expression profiles. *Proc Natl Acad Sci U S A* 2005;**102**:15545–50
17. Mootha VK, Lindgren CM, Eriksson KF, Subramanian A, Sihag S, Lehar J, Puigserver P, Carlsson E, Ridderstrale M, Laurila E, Houstis N, Daly MJ, Patterson N, Mesirov JP, Golub TR, Tamayo P, Spiegelman B, Lander ES, Hirschhorn JN, Altshuler D, Groop LC. PGC-1alpha-responsive genes involved in oxidative phosphorylation are coordinately downregulated in human diabetes. *Nat Genet* 2003;**34**:267–73
18. Gene Ontology C Gene ontology consortium: going forward. *Nucleic Acids Res* 2015;**43**:D1049–56
19. The Gene Ontology C The gene ontology resource: 20 years and still going strong. *Nucleic Acids Res* 2019;**47**:D330–D38
20. Kanehisa M, Sato Y, Kawashima M, Furumichi M, Tanabe M. KEGG as a reference resource for gene and protein annotation. *Nucleic Acids Res* 2016;**44**:D457–62
21. Jenne CN, Kubes P. Immune surveillance by the liver. *Nat Immunol* 2013;**14**:996–1006
22. Racanelli V, Rehermann B. The liver as an immunological organ. *Hepatology* 2006;**43**:S54–62
23. Bindea G, Mlecnik B, Tosolini M, Kirilovsky A, Waldner M, Obenauf AC, Angell H, Fredriksen T, Lafontaine L, Berger A, Bruneval P, Fridman WH, Becker C, Pages F, Speicher MR, Trajanoski Z, Galon J. Spatiotemporal dynamics of intratumoral immune cells reveal the immune landscape in human cancer. *Immunity* 2013;**39**:782–95
24. Garnelo M, Tan A, Her Z, Yeong J, Lim CJ, Chen J, Lim KH, Weber A, Chow P, Chung A, Ooi LL, Toh HC, Heikenwalder M, Ng IO, Nardin A, Chen Q, Abastado JP, Chew V. Interaction between tumour-infiltrating B cells and T cells controls the progression of hepatocellular carcinoma. *Gut* 2017;**66**:342–51
25. Tian Z, Hou X, Liu W, Han Z, Wei L. Macrophages and hepatocellular carcinoma. *Cell Biosci* 2019;**9**:79
26. van der Leun AM, Thommen DS, Schumacher TN. CD8(+) T cell states in human cancer: insights from single-cell analysis. *Nat Rev Cancer* 2020;**20**:218–32
27. Ding W, Xu X, Qian Y, Xue W, Wang Y, Du J, Jin L, Tan Y. Prognostic value of tumor-infiltrating lymphocytes in hepatocellular carcinoma: a meta-analysis. *Medicine* 2018;**97**:e13301
28. Sangro B, Gomez-Martin C, de la Mata M, Inarrairaegui M, Garralda E, Barrera P, Riezu-Boj JI, Larrea E, Alfaro C, Sarobe P, Lasarte JJ, Perez-Gracia JL, Melero I, Prieto J. A clinical trial of CTLA-4 blockade with tremelimumab in patients with hepatocellular carcinoma and chronic hepatitis C. *J Hepatol* 2013;**59**:81–8
29. Kambhampati S, Bauer KE, Bracci PM, Keenan BP, Behr SC, Gordan JD, Kelley RK. Nivolumab in patients with advanced hepatocellular carcinoma and Child-Pugh class B cirrhosis: safety and clinical outcomes in a retrospective case series. *Cancer* 2019;**125**:3234–41
30. Egeblad M, Littlepage LE, Werb Z. The fibroblastic coconspirator in cancer progression. *Cold Spring Harb Symp Quant Biol* 2005;**70**:383–8
31. Lee NH, Nikfarjam M, He H. Functions of the CXC ligand family in the pancreatic tumor microenvironment. *Pancreatology* 2018;**18**:705–16
32. Zhang J, Chen J, Guan GW, Zhang T, Lu FM, Chen XM. [Expression and clinical significance of chemokine CXCL10 and its receptor CXCR3 in hepatocellular carcinoma.]. *Beijing Da Xue Xue Bao Yi Xue Ban* 2019;**51**:402–8
33. Tokunaga R, Zhang W, Naseem M, Puccini A, Berger MD, Soni S, McSkane M, Baba H, Lenz HJ. CXCL9, CXCL10, CXCL11/CXCR3 axis for immune activation – a target for novel cancer therapy. *Cancer Treat Rev* 2018;**63**:40–7
34. Ren T, Zhu L, Cheng M. CXCL10 accelerates EMT and metastasis by MMP-2 in hepatocellular carcinoma. *Am J Transl Res* 2017;**9**:2824–37
35. Ghanem I, Riveiro ME, Paradis V, Faivre S, de Parga PM, Raymond E. Insights on the CXCL12-CXCR4 axis in hepatocellular carcinoma carcinogenesis. *Am J Transl Res* 2014;**6**:340–52
36. Castro A, Ozturk K, Pyke RM, Xian S, Zanetti M, Carter H. Elevated neoantigen levels in tumors with somatic mutations in the HLA-A, HLA-B, HLA-C and B2M genes. *BMC Med Genomics* 2019;**12**:107
37. del Campo AB, Kyte JA, Carretero J, Zinchencko S, Mendez R, Gonzalez-Aseguinolaza G, Ruiz-Cabello F, Aamdal S, Gaudernack G, Garrido F, Aptsiauri N. Immune escape of cancer cells with beta2-microglobulin loss over the course of metastatic melanoma. *Int J Cancer* 2014;**134**:102–13
38. Sun J, Yang ZL, Miao X, Zou Q, Li J, Liang L, Zeng G, Chen S. ATP5b and beta2-microglobulin are predictive markers for the prognosis of patients with gallbladder cancer. *J Mol Hist* 2015;**46**:57–65
39. Ouda SM, Khairy AM, Sorour AE, Mikhail MN. Serum beta-2 microglobulin: a possible marker for disease progression in Egyptian patients with chronic HCV related liver diseases. *Asian Pac J Cancer Prev* 2015;**16**:7825–9

(Received June 5, 2020, Accepted October 8, 2020)